AEM
Journals.ASM.org

Metabolic Pathway Involved in 2-Methyl-6-Ethylaniline Degradation by *Sphingobium* sp. Strain MEA3-1 and Cloning of the Novel Flavin-Dependent Monooxygenase System *meaBA*

Weiliang Dong,[a] Qiongzhen Chen,[a] Ying Hou,[b] Shuhuan Li,[a] Kai Zhuang,[a] Fei Huang,[a] Jie Zhou,[a] Zhoukun Li,[a] Jue Wang,[a] Lei Fu,[a] Zhengguang Zhang,[d] Yan Huang,[a] Fei Wang,[c] Zhongli Cui[a]

Key Laboratory of Agricultural Environmental Microbiology, Ministry of Agriculture, College of Life Sciences, Nanjing Agricultural University, Nanjing, People's Republic of China[a]; College of Food and Bioengineering, Henan University of Science and Technology, Luoyang, People's Republic of China[b]; College of Bioscience and Bioengineering, Jiangxi Agricultural University, Nanchang, People's Republic of China[c]; College of Plant Protection, Nanjing Agricultural University, Nanjing, People's Republic of China[d]

2-Methyl-6-ethylaniline (MEA) is the main microbial degradation intermediate of the chloroacetanilide herbicides acetochlor and metolachlor. *Sphingobium* sp. strain MEA3-1 can utilize MEA and various alkyl-substituted aniline and phenol compounds as sole carbon and energy sources for growth. We isolated the mutant strain MEA3-1Mut, which converts MEA only to 2-methyl-6-ethyl-hydroquinone (MEHQ) and 2-methyl-6-ethyl-benzoquinone (MEBQ). MEA may be oxidized by the P450 monooxygenase system to 4-hydroxy-2-methyl-6-ethylaniline (4-OH-MEA), which can be hydrolytically spontaneously deaminated to MEBQ or MEHQ. The MEA microbial metabolic pathway was reconstituted based on the substrate spectra and identification of the intermediate metabolites in both the wild-type and mutant strains. Plasmidome sequencing indicated that both strains harbored 7 plasmids with sizes ranging from 6,108 bp to 287,745 bp. Among the 7 plasmids, 6 were identical, and pMEA02′ in strain MEA3-1Mut lost a 37,000-bp fragment compared to pMEA02 in strain MEA3-1. Two-dimensional electrophoresis (2-DE) and protein mass fingerprinting (PMF) showed that MEA3-1Mut lost the two-component flavin-dependent monooxygenase (TC-FDM) MeaBA, which was encoded by a gene in the lost fragment of pMEA02. MeaA shared 22% to 25% amino acid sequence identity with oxygenase components of some TC-FDMs, whereas MeaB showed no sequence identity with the reductase components of those TC-FDMs. Complementation with *meaBA* in MEA3-1Mut and heterologous expression in *Pseudomonas putida* strain KT2440 resulted in the production of an active MEHQ monooxygenase.

Chloroacetanilide herbicides are widely used throughout the world (1) for the control of most annual grasses and certain broadleaf weeds (2). The majority of the commonly used chloroacetanilide herbicides, such as alachlor, acetochlor, butachlor, and metolachlor, are *N*-alkoxyalkyl-*N*-chloroacetyl-substituted aniline derivatives (3). Long-term application of these herbicides has caused negative impacts on both the aquatic environment and agricultural ecosystems (4, 5). Acetochlor has been classified by the U.S. Environmental Protection Agency (EPA) (4) as a B-2 carcinogen and a probable human carcinogen, and several chloroacetanilide herbicides have been proven to cause tumors in rats (6). Thus, there is great concern about the behavior and fate of chloroacetamide herbicides and their degradation metabolites in the environment.

Although chloroacetamide herbicides may be degraded through chemical and physical processes, microbial metabolism is the main mechanism responsible for herbicidal degradation in natural soils (7, 8). A variety of bacterial strains that are able to degrade butachlor, alachlor, acetochlor, and metolachlor have been characterized (9, 10). In the degradation pathway, these herbicides are *N*-dealkylated to 2-chloro-*N*-(2,6-diethylphenyl) acetamide (CDEPA) (for alachlor and butachlor) or 2-chloro-*N*-(2-methyl-6-ethylphenyl) acetamide (CMEPA) (for acetochlor and metolachlor), which are then converted to 2,6-diethylaniline (DEA) or 2-methyl-6-ethylaniline (MEA), respectively (2, 10). Oxygenase systems are involved in bacterial degradative *N*-dealkylation. A novel three-component Rieske non-heme iron oxygenase system was determined to catalyze the *N*-dealkylation of chloroacetamide herbicides in *Sphingomonas* sp. strains DC-6 and DC-2 (3). A cytochrome P450 system, EthBAD, was reported to be involved in the *N*-deethoxymethylation of acetochlor by *Rhodococcus* sp. strain T3-1 (11). Two genes, *cmeH* and *damH*, were cloned from *Sphingobium quisquiliarum* strain DC-2 and *Delftia* sp. strain T3-6, respectively, and were shown to encode amidases that catalyze the amide bond cleavage of CDEPA or CMEPA to DEA or MEA, respectively (10, 12).

Alkyl substituents of the aniline derivatives of MEA are located on both sides of the amine group. This special chemical structure makes MEA more difficult to be degraded in natural soils (13). Under conditions of both batch and continuous operations, an oxidation pathway for 2,6-dimethylaniline (DMA) via hydroxyl

Received 9 June 2015 **Accepted** 11 September 2015

Accepted manuscript posted online 18 September 2015

Citation Dong W, Chen Q, Hou Y, Li S, Zhuang K, Huang F, Zhou J, Li Z, Wang J, Fu L, Zhang Z, Huang Y, Wang F, Cui Z. 2015. Metabolic pathway involved in 2-methyl-6-ethylaniline degradation by *Sphingobium* sp. strain MEA3-1 and cloning of the novel flavin-dependent monooxygenase system *meaBA*. Appl Environ Microbiol 81:8254–8264. doi:10.1128/AEM.01883-15.

Editor: F. E. Löffler

Address correspondence to Zhongli Cui, czl@njau.edu.cn.

W.D. and Q.C. contributed equally to this work.

Supplemental material for this article may be found at http://dx.doi.org/10.1128/AEM.01883-15.

TABLE 1 Strains and plasmids used in this study

Strain or plasmid	Characteristic(s)[a]	Source or reference
Strains		
Sphingobium sp. MEA3-1	Wild-type MEA degrader, pMEA01–pMEA07, Sm^r	2
Sphingobium sp. MEA3-1Mut	Derivative of MEA3-1, deletion within pMEA02	This study
P. putida KT2440	A model strain for aromatic catabolism, Cm^r Amp^r	31
E. coli DH5α	Host strain for cloning vectors	TaKaRa
E. coli HB101(pRK600)	Conjugation helper strain, Cm^r	33
Plasmids		
pBBR1MCS-2	Broad-host-range cloning vector, Km^r	30
pBBR-meaA	pBBR1MCS-5 derivative carrying *meaA*, Km^r	This study
pBBR-meaBA	pBBR1MCS-5 derivative carrying *meaBA*, Km^r	This study
pBBR-meaBA-orf1-4	pBBR1MCS-5 derivative carrying 7,479 bp	This study
pET29a-meaBAT7	pET29a(+) derivative carrying *meaBA*, Km^r	This study
pMD19-T	T-A cloning vectors, Amp^r	TaKaRa

[a] Sm^r, streptomycin resistant; Cm^r, chloramphenicol resistant; Amp^r, ampicillin resistant; Km^r, kanamycin resistant.

radicals ($OH^{\bullet}$) was proposed to use Fenton's reactions, in which 2,6-dimethyl-phenol (DMP), 2,6-dimethyl-hydroquinone (DMHQ), 2,6-dimethyl-*p*-benzoquinone (DMBQ), and 3-hydroxy-2,6-dimethyl-*p*-benzoquinone (3-OH-DMBQ) were detected as aromatic by-products (13). Chao et al. (14) reported that DMA was transformed to 4-hydroxy-2,6-dimethylaniline (4-OH-DMA) by a P450 monooxygenase system in cultured mammalian cells. *Sphingobium baderi* strain DE-13 is capable of degrading MEA to the intermediate 4-OH-MEA, which is further transformed to 2-methyl-6-ethyl-benzoquinone imine (MEBQI) (10). Zhang et al. (9) proposed a DEA dealkylation process during the degradation of butachlor by *Paracoccus* sp. strain FLY-8. However, the molecular basis of and further metabolic pathways for DEA, MEA, DMA, and DMP in microorganisms remain unclear.

The biochemical pathway of acetochlor degradation by a three-bacterium consortium was proposed (acetochlor to CMEPA by *Rhodococcus* sp. strain T3-1, CMEPA to MEA by *Delftia* sp. strain T3-6, and MEA by *Sphingobium* sp. strain MEA3-1) based on the identified degradation intermediates (2). Recently, acetochlor and CMEPA metabolisms have been described in *Rhodococcus* sp. T3-1 and *Delftia* sp. T3-6 (11, 12). In this study, we clarified the partial metabolic pathway responsible for MEA degradation and cloned a novel flavin-dependent monooxygenase system, MeaBA, involved in MEA degradation.

MATERIALS AND METHODS

Chemicals and media. MEA was purchased from Qingdao Vochem Co., Ltd. (Qingdao, China), and 4-OH-DMA and DMHQ (structural analogues of 4-OH-MEA and MEHQ, respectively) were purchased from Sigma-Aldrich (Shanghai, China). Other alkyl-substituted aniline or phenol compounds were purchased from Sinopharm Chemical Reagent Co., Ltd. (Beijing, China). All molecular reagents were purchased from TaKaRa Co., Ltd. (Dalian, China). All chemicals used in this study were of analytical grade or higher purity. Minimal salts medium (MSM), lysogeny broth (LB) medium, and 1/3 LB medium were used for the strains cultured in this study (15).

Bacterial strains, plasmids, and culture conditions. The strains, plasmids, and primers used in this study are listed in Tables 1 and 2. *Escherichia coli* strains were routinely grown aerobically at 37°C and 180 rpm in LB medium. Strains MEA3-1 and MEA3-1Mut were grown aerobically at 30°C and 180 rpm in 1/3 LB medium (16), unless otherwise indicated. *Pseudomonas putida* strain KT2440 was grown aerobically at 30°C and 180 rpm in LB medium.

Isolation of spontaneous mutant strains. *Sphingobium* sp. MEA3-1 (China Center for Type Culture Collection [CCTCC] M 2012527) was cultured on 1/3 LB plates without selection, and isolated colonies were transferred to fresh 1/3 LB plates. After continuous transfers, colonies with different morphotypes were observed and purified. The ability of the resulting isolates to degrade MEA was determined, as described below. The mutant strain that lost the ability to mineralize MEA was designated MEA3-1Mut. The enterobacterial repetitive intergenic consensus PCR (ERIC-PCR) pattern (17) and 16S rRNA gene sequence of strain MEA3-1Mut were determined and compared with those of the wild-type strain MEA3-1.

Degradation experiment. The wild-type and mutant strains were cultured in 1/3 LB medium, harvested by centrifugation (Allegra X-22R centrifuge, F0630 rotor; Beckman Coulter, USA) at 2,180 × *g* and 4°C for 10 min, washed twice with fresh MSM, and then resuspended in MSM to an approximate optical density at 600 nm (OD_{600}) of 2.0 as the inoculum. The 1.0-ml inocula of wild-type and mutant strains were inoculated into a 100-ml Erlenmeyer flask containing 50 ml of MSM supplemented with 100 mg/liter different aromatic compounds as the sole carbon sources at

TABLE 2 Primers used in this study

Primer	Sequence (5′ to 3′)[a]	Target gene(s)
MeaBp-F	CTCGAGGATCGGCCATCCTATCGCTG	
MeaA-R	GAGCTCTCATCGCGCCTCCGTCAGCGC	*meaBA*
MeaAp-F	CTCGAGGATCGGCCATCCTATCGCTGAACAGCTTCGGCGGTAT CTAGAGGAGGTACTTTGAATGGAAGAGGCGCATAACAA	*meaA* (fusion promoter sequence)
Orf4-R	GAGCTCCTAACAATCCACCCGGACCA	*meaBA-orf1-4*
16S-F	GCGTAGGATTAGCTAGTTGGT	Partial 16S rRNA sequence
16S-R	AGCTAGTTATCATCGTTTACG	Partial 16S rRNA sequence

[a] Restriction sites are underlined.

180 rpm and 30°C, respectively. These aromatic compounds included phenol and the aniline derivatives DEA, DMA, aniline, 2,3-dimethylaniline (2,3-DMA), 2,4-dimethyl-aniline (2,4-DMA), DMHQ, 4-OH-DMA, 2-methyl-aniline (2-MA), toluene, *O*-xylene, phenol, catechol, hydroxyquinol, 2-methyl-phenol (2-MP), 2,6-dimethyl-phenol (2,6-DMP), 3,5-dimethyl-phenol (3,5-DMP), and 3,4-dimethyl-phenol (3,4-DMP). The degradation of these aromatic compounds was measured using high-performance liquid chromatography (HPLC). All treatments were performed in triplicate, and control experiments without inoculation or without substrates were performed under the same conditions.

Identification of MEA-degrading metabolites. The 2.0-ml inocula of strains MEA3-1 and MEA3-1Mut, as described above, were inoculated into a 250-ml Erlenmeyer flask containing 100 ml of MSM supplemented with 100 mg/liter MEA. When the concentration of MEA decreased to approximately 50 mg/liter, the supernatant was collected by centrifugation at 12,580 × *g* and 4°C for 10 min and lyophilized. The residual was dissolved in 1 ml of methanol, which was filtered through a 0.22-μm-pore-size Millipore membrane (Sangon Biotech, Shanghai, China) for HPLC-tandem mass spectrometry (HPLC-MS/MS) analysis. A 5-μm C_{18} separation column (internal diameter, 4.6 mm; length, 250 mm) filled with Kromasil 100 Å was used for HPLC analysis. The mobile phase was methanol-water (80:20 [vol/vol]), and the flow rate was 0.8 ml/min. The detection wavelength was 240 nm, and the injection volume was 20 μl. MS analysis was performed in electrospray ionization (ESI) mode with an Agilent G6410B triple-quad mass spectrometer. In the MS analysis, the metabolites were separated and ionized by electrospray ionization to obtain a positive polarity. Characteristic fragment ions were identified by second-order MS and compared to those generated with authentic or structural analogue standards.

Plasmid profiling. Plasmids from strains MEA3-1 and MEA3-1Mut were isolated using a modified alkaline extraction method (18). After 12 h of incubation (logarithmic phase), approximately 5×10^9 cells were harvested by centrifugation at 12,580 × *g* and 4°C for 10 min and resuspended in 1.0 ml of buffer I (1 M NaCl and 50 mM glucose in Tris-EDTA [TE] buffer [pH 8.0]) after they were washed with 5 ml of TE buffer (10 mM Tris-HCl, 1 mM EDTA [pH 8.0]). The cells were incubated with 20 μg/ml RNase and 100 μg/ml lysozyme at 37°C for 30 min until the cells began to lyse. Next, 2.0 ml of freshly prepared buffer II (0.2 M NaOH, 10 g/liter SDS) was added and mixed gently. The samples were placed on ice for 15 min. Next, 1.5 ml of ice-cold buffer III (5 M potassium acetate, 11.5% acetic acid [vol/vol]) was added and mixed gently until a white precipitate formed. The supernatant was collected by centrifugation at 12,580 × *g* and 4°C for 15 min. Other procedures and manipulations (phenol-chloroform extraction and isopropanol precipitation) were operated as described by O'Sullivan and Klaenhammer (18).

The isolated plasmids were visualized using pulsed-field gel electrophoresis (PFGE) (Bio-Rad) (19). PFGE was performed in TBE buffer (20 mM Tris-HCl, 20 mM boric acid, 0.5 mM EDTA [pH 8.0]) at 12.5°C at 6 V/cm, with linearly increasing pulse times from 10 to 20 s for 24 h. HindIII-digested lambda phage DNA was used as a molecular size standard.

Plasmidome sequencing, assembly, and annotation. The plasmids from strains MEA3-1 and MEA3-1Mut were isolated, as described above, and the linear DNA in the plasmidomes was digested using ATP-dependent DNase. The 16S-F/16S-R primer pair, which targets the 16S rRNA gene, was used to detect residual chromosomal DNA. The plasmidomes of strains MEA3-1 and MEA3-1Mut were shotgun sequenced (20) with a Roche 454 genome sequencer FLX Titanium platform (Han-Yu Biological Technology Co. Ltd.) (21). The sequencing depth and the fold coverage of the plasmid draft were 20× and 99-fold, respectively. Sequencing reads were assembled using the SOAP*denovo* software (version 1.05; http://soap.genomics.org.cn/soapdenovo.html). *De novo* gene prediction was conducted using Glimmer (version 3.0; http://ccb.jhu.edu/software/glimmer/index.shtml). The BLAST program (22), combined with sequences from the KEGG, COG, Swiss-Prot, and nonredundant protein databases, was used to accomplish functional annotation, with an *E* value cutoff of $1E^{-5}$.

The gaps predicted by MUMmer and BLAST were closed using ContigScape (23), which interactively displayed the relationships between plasmidome contigs, thereby allowing a faster and more precise determination of linkages and greatly improving the efficiency of gap closure (23). Gap closure was verified by PCR and self-formed adaptor PCR (SEFA PCR) (24) amplification; all gap closure primers are shown in Table S1 in the supplemental material.

Protein extraction and 2-DE analysis. Crude enzyme extracts of strains MEA3-1 and MEA3-1Mut were prepared using ultrasonic disruption (Sonicator 201 M; Kubota, Japan) for 10 min at 4°C in a lysis buffer {7 M urea, 2 M thiourea, 4% (wt/vol) 3-[(3-cholamidopropyl)-dimethylammonio]-1-propanesulfonate (CHAPS), 0.2% (wt/vol) Bio-Lyte (Bio-Rad) (pH 3 to 10), 65 mM dithiothreitol (DTT)} and centrifuged at 12,580 × *g* at 4°C for 20 min to remove cell debris. Protein concentrations were determined using a modified Bradford assay (25), with ovalbumin as the standard.

The proteins in the supernatant were analyzed using 2-DE. For each replicate, 100 μg of total protein extract was loaded onto 17-cm immobilized pH gradient dry strips (pH 4 to 7 linear gradient; Bio-Rad, USA) during the rehydration step (13 h), followed by focusing for a total of 60,000 V · h using a Protean isoelectric focusing (IEF) cell (Bio-Rad). After isoelectric focusing, the gel strips were equilibrated in 5 ml of equilibration buffer (0.375 M Tris-HCl [pH 8.8], 6 M urea, 20% [vol/vol] glycerol, 2% [wt/vol] SDS, and 2% [wt/vol] DTT) for 15 min and then reequilibrated for 15 min in the same buffer but without DTT, which was replaced with iodoacetamide (2.5% [wt/vol]) (26). SDS-PAGE in the second dimension was performed with 12% SDS-polyacrylamide gels (25 cm by 20 cm) and sealed with low-melting-point agarose (0.5% [wt/vol]). Electrophoresis was performed using a Protean Plus Dodeca cell apparatus (Bio-Rad) at 50 V for the first 30 min, followed by 150 V for 8 h. The protein spots were visualized using mass spectrometry-compatible silver staining (27).

Protein mass fingerprinting (PMF). The gels were scanned using a Umax PowerLook III scanner (Umax Technologies, USA) at a resolution of 300 dots per in. (dpi), and the images of the gels were analyzed with PDQuest (version 8.0; Bio-Rad). Selected protein spots were manually excised from the gels for matrix-assisted laser desorption ionization–time of flight mass spectrometry (MALDI-TOF MS) analysis (Bo-Yuan Biological Technology Co. Ltd.). The resulting peptide fragments were analyzed by searching against the plasmidome databases of strains MEA3-1 and MEA3-1Mut, as described below.

Cloning of *meaBA*. The lost genes in *Sphingobium* sp. strain MEA3-1 that may be involved in MEA degradation were analyzed in detail by searching against the NCBI database and the Protein Data Bank (PDB). Possible monooxygenase genes involved in MEA degradation, designated *meaBA*, were further studied by sequence analysis and functional verification, as described below.

For phylogenetic analysis, the amino acid sequences of MeaA and MeaB were first aligned using Clustal X (version 2.1) (28) and then imported into MEGA (version 5.0) (29) to construct a phylogenetic tree via the neighbor-joining method. Distances were calculated using the Kimura two-parameter distance model. Confidence values for the branches of the phylogenetic tree were determined using bootstrap analysis based on 1,000 resamplings.

Functional complementation of MEA3-1Mut and KT2440 with MeaBA. Genomic DNA was extracted and purified from strain MEA3-1 via high-salt precipitation (11). Three PCR fragments (1,224 bp, 2,069 bp, and 6,247 bp) containing the 60-bp potential promoter region of *meaB* were amplified using the primer pairs MeaAp-F/MeaA-R, MeaBp-F/MeaA-R, and MeaBp-F/Orf4-R (Table 2), designated *meaA*, *meaBA*, and *meaBA-orf1-4* (i.e., *meaBA* with *orf1* to *orf4*), respectively. The three fragments were digested with SacI and XhoI and inserted into the corresponding sites of the broad-host-range plasmid pBBR1MCS-2 (30) to gener-

ate pBBR-meaA, pBBR-meaBA, and pBBR-meaBA-orf1-4, respectively. The inserted fragments in the three plasmids were verified by sequencing. The resulting three plasmids were transformed into *E. coli* DH5α. Next, three plasmids were introduced into strains MEA3-1Mut and KT2440 (31) via triparental mating (32), using pRK600 (33) as the helper plasmid. The abilities of the strains harboring different plasmids to degrade MEA and MEHQ were determined using a whole-cell biotransformation assay, as described by Liu et al. (34). Samples were taken at regular intervals, the concentrations of the substrates were determined rapidly using a UV-visible spectrophotometer, and bacterial growth was monitored by measuring the CFU (CFU per milliliter).

Effect of metyrapone on the degradation of MEA. Metyrapone is a specific inhibitor of cytochrome P450 monooxygenase systems (35). Therefore, 200 μl of MSM containing 0.5 mM MEA and different concentrations of metyrapone (100 mg/liter, 200 mg/liter, and 300 mg/liter) were added into 96-well plates inoculated with strain MEA3-1. The concentration of MEA was measured by color development with 4-aminoantipyrene and potassium hexacyanoferrate (12). Reaction mixtures without inoculation and metyrapone were used as negative and positive controls, respectively.

Simulation of 4-OH-MEA hydrolytic deamination. 4-OH-DMA, a structural analogue of 4-OH-MEA, was used to simulate the spontaneous hydrolytic deamination process. Briefly, 200 μl of pure water containing 0.5 mM 4-OH-DMA was added to 96-well plates, and Nessler's reagent was added at intervals to determine the release of ammonia (36).

Nucleotide sequence accession numbers. The GenBank accession number of the 12,052-bp DNA fragment containing the *meaBA* gene cluster and *orf1-9* is KP752077. The sequence of the plasmidome from *Sphingobium* sp. strain MEA3-1 has been deposited in GenBank under the accession numbers CM003352 to CM003358. The accession numbers for the oxygenase components are in the legend to Fig. 4.

RESULTS

Isolation of MEA degradation-deficient mutants and metabolite identification. The MEA degradation phenotype of *Sphingobium* sp. strain MEA3-1 was quite unstable. Large and small colonies appeared when the inoculum was freshly streaked from samples frozen at −80°C or after continuous transfers on 1/3 LB medium without selective pressure. The 16S rRNA gene sequence of the mutant strain exhibited 100% similarity with that of strain MEA3-1. The ERIC-PCR (17, 37) patterns of the two strains exhibited identical fragment distributions (see Fig. S1 in the supplemental material). These results indicated that the larger-size colony was indeed an MEA degradation-deficient mutant of strain MEA3-1 and was designated *Sphingobium* sp. strain MEA3-1Mut.

Strain MEA3-1 was able to completely degrade MEA, as detected by HPLC analysis, and to utilize MEA as the sole carbon source for growth (2). However, the whole-cell transformation experiments indicated that strain MEA3-1Mut could transform MEA only into an unidentified metabolite (Fig. 1). The MS/MS results indicated that the MEA substrate, with a retention time (t_R) of 5.68 min, has a prominent protonated molecular ion at *m/z* 136 and fragment ions of *m/z* 120, 108, and 91 (Fig. 1A). Product A, with a t_R of 5.08 min, has a molecular ion at *m/z* 152 and fragment ions of *m/z* 135, 123, and 107, which correspond to a hydroxylated form of MEA (Fig. 1C). Product A was proposed to be 4-hydroxy-2-methyl-6-ethylaniline (4-OH-MEA). Product B, with a t_R of 4.61 min, has a molecular ion at *m/z* 153 and fragment ions of *m/z* 136, 121, and 108, which correspond to the hydrolytic deamination of product A (Fig. 1B). Product B was proposed to be 2-methyl-6-ethyl-hydroquinone (MEHQ). The possible spontaneous oxidation products of 4-OH-MEA and MEHQ, 2-methyl-6-ethyl-benzoquinone imine (MEBQI) at *m/z* 150 and 2-methyl-6-ethyl-benzoquinone (MEBQ) at *m/z* 151, respectively, were also detected using HPLC-MS (data not shown). The MS/MS fragment results were analyzed based on the compound structures (Fig. 1).

Identification of MEA-degrading metabolites from strain MEA3-1. *Sphingobium* sp. strain MEA3-1 can utilize MEA as a sole carbon and energy source but cannot utilize aniline for growth (38), indicating that strain MEA3-1 employs different pathways to degrade alkyl-substituted aniline compounds. To clarify the MEA degradation pathway in this strain, the degradation intermediates were analyzed. Using HPLC-MS, the same degradation products, 4-OH-MEA and MEHQ, were detected in the culture medium extracts of strain MEA3-1 during the biodegradation of MEA (data not shown). Another metabolite, product C (t_R, 2.70 min), exhibited a molecular ion at *m/z* 169 and fragment ions of *m/z* 152, 134 and 115.7, which correspond to the hydroxylated form of MEHQ. Product C was proposed to be 3-hydroxy-2-methyl-6-ethyl-hydroquinone (3-OH-MEHQ) (Fig. 1D), and the possible spontaneous oxidation product 3-hydroxy-2-methyl-6-ethyl-benzoquinone (3-OH-MEBQ), with a molecular ion of *m/z* 167 and the same MS/MS fragment ions, was also detected.

In addition to 4-OH-MEA, MEHQ was detected in the MEA metabolites. We speculate that MEBQI, the 4-OH-MEA oxidation product, can spontaneously hydrolytically deaminate to MEBQ or MEHQ. 4-OH-DMA, a structural analogue of 4-OH-MEA, was used to simulate the spontaneous hydrolytic deamination process using Nessler's reagent colorimetry. As shown in Fig. S2 in the supplemental material, 4-OH-DMA was rapidly spontaneously deaminated by hydrolysis in pure water. Considering the similar structures of 4-OH-MEA and 4-OH-DMA, a similar reaction may also occur with 4-OH-MEA.

The substrate degradation spectra of the wild-type and mutant strains. Using HPLC analysis, the degradation of alkyl-substituted aniline or phenol compounds by wild-type and mutant strains was monitored. The degradation results are shown in Table 3. Wild-type strain MEA3-1 degraded most alkyl-substituted aniline or phenol compounds, except for toluene, xylene, aniline, 2,3-DMA, 2,4-DMA, and 3,4-DMP. These results indicated that strain MEA3-1 employs different pathways to degrade alkyl-substituted aniline compounds, and this metabolic pathway is similar to that of alkyl-substituted phenol compounds. However, the mutant strain MEA3-1Mut was able to transform only alkyl-substituted aniline and phenol compounds; it is worth noting that the mutant strain did not degrade 4-OH-DMA and DMHQ, which are structural analogues of 4-OH-MEA and MEHQ, respectively. These results indicate that the degradation of MEA by strain MEA3-1 is subject to *para*-hydroxylation of the ring. Given the MEA-degrading metabolites of strains MEA3-1 and MEA3-1Mut, a possible pathway for MEA degradation by *Sphingobium* sp. MEA3-1 is illustrated in Fig. 2, and MEA3-1Mut has likely lost a key gene or gene cluster for MEBQ degradation.

Plasmidome sequencing. Considering the unstable degradative phenotype, we deduced that the genes encoding the MEA-degrading enzymes were located on plasmids. The plasmid profiles of MEA3-1 and MEA3-1Mut were analyzed using PFGE. Seven plasmids, designated pMEA01, pMEA02 (pMEA02′ for strain MEA3-1Mut), pMEA03, pMEA04, pMEA05, pMEA06, and pMEA07, were detected (Fig. 3). By comparing the plasmid profiles of strains MEA3-1 and MEA3-1Mut, six of the seven plasmids were found to shift identically during the PFGE of both strains. Compared with its counterpart pMEA02 in strain MEA3-1, a

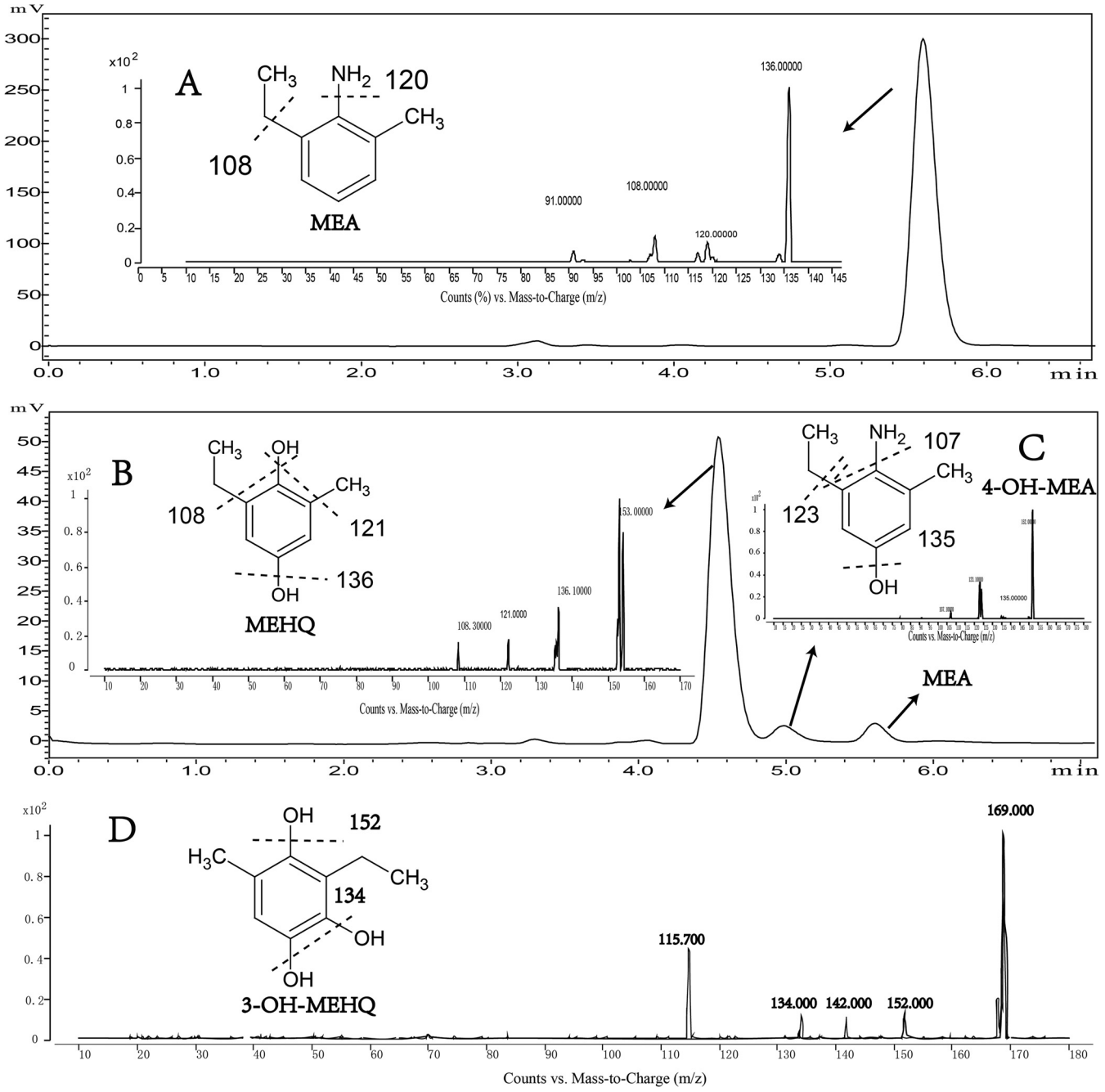

FIG 1 HPLC and mass spectrum detection of the intermediate metabolites. (A to D) HPLC and positive-ion mass spectra of the substrate MEA (A), of the metabolite product (MEHQ) by strain MEA3-1Mut (B), of the metabolite product (4-OH-MEA) by strain MEA3-1Mut (C), and of the metabolite product (3-OH-MEHQ) by strain MEA3-1 (D).

smaller plasmid, pMEA02′, was observed in the mutant (Fig. 3). We deduced that pMEA02′ is a derivative of pMEA02, with some portions deleted.

The plasmidomes of strains MEA3-1 and MEA3-1Mut were sequenced and subjected to gap closure. The total number of contigs of strain MEA3-1 was 213, with a total length of 785,046 bp. Gaps between the contigs were closed via bioinformatic analysis and primer walking with PCR products. Seven complete plasmid sequences (pMEA01 to pMEA07) were obtained, and a circle graph of pMEA02 from strain MEA3-1 is shown in Fig. S3 in the supplemental material.

The largest and smallest plasmids were 287,745 bp and 6,108 bp, with 413 and 10 open reading frames (ORFs), respectively. The seven plasmids were not homologous to other large plasmids from *Sphingomonas* spp., and most of the ORFs were annotated as hypothetical proteins, plasmid-relevant proteins, or transposases. The 134,691-bp pMEA02 plasmid contained 164 ORFs with six IS*6100* transposase regions and many other transposase family regions. A

TABLE 3 Substrate spectra of strains MEA3-1 and MEA3-1Mut

Substrate	Result with[a]:	
	MEA3-1	MEA3-1Mut
MEA	+	*
DEA	+	*
DMA	+	*
Aniline	−	−
2,3-DMA	−	−
2,4-DMA	−	−
2-MA	+	*
4-OH-DMA	+	−
DMHQ	+	−
Toluene	−	−
O-Xylene	−	−
Phenol	+	+
Catechol	+	+
Hydroxyquinol	+	+
Hydroquinone	+	+
2-MP	+	*
2,6-DMP	+	*
3,5-DMP	+	*
3,4-DMP	−	−

[a] +, positive for strain growth and substrates were degraded; −, negative for strain growth and substrates were not degraded; *, negative for strain growth and substrates were transformed to other compounds. The biomass was measured at 600 nm (OD_{600}) using a Shimadzu UV-visible spectrophotometer. The mineralization or cometabolic transformation of these aromatic compounds was measured using HPLC, all treatments were performed in triplicate, and control experiments without inoculation and without substrate were performed under the same conditions.

24,948-bp fragment (from bp 132840 to 23097 in pMEA02) and a 12,052-bp fragment (from bp 43824 to 55875 in pMEA02) were lost to generate the plasmid pMEA02′ in strain MEA3-1Mut (see Fig. S3). Therefore, MEA degradation-related genes may be located in these contigs in pMEA02 from strain MEA3-1.

2-DE and PMF analyses. *Sphingobium* sp. strains MEA3-1 and MEA3-1Mut total proteins were analyzed using 2-DE to determine the differences associated with pMEA02 in the wild-type and mutant strains. As revealed by PDQuest software analysis, the protein profiles produced from the 2-DE gels were highly reproducible among the three independent extractions. Figure S4 in the supplemental material shows representative gels of the soluble proteins extracted from strains MEA3-1 and MEA3-1Mut. Compared with MEA3-1Mut, strain MEA3-1 had three significantly distinct protein spots, which were designated A, B, and C.

PMF analysis identified several peptide fragments from the three protein spots (see Table S2 in the supplemental material). Genes encoding the three proteins were located at bp 9382 to 10158, bp 12713 to 13816, and bp 45926 to 47104 in pMEA02, which were lost in MEA3-1Mut. The three proteins exhibited 100%, 99%, and 99% amino acid sequence similarity with 3-hydroxy-2-methylbutyryl-coenzyme A (CoA) dehydrogenase (spot A), acyl-CoA dehydrogenase (ACAD) (spot B), and hypothetical protein (spot C) from *Sphingomonas* sp. DC-6, respectively, as determined by searching against the NCBI protein database. It is worth noting that the strain DC-6 was reported to completely mineralize acetochlor (3, 10).

ORF analysis. Spots A and B are located in the lost 24,948-bp fragment, and spot C is located in the lost 12,052-bp fragment. The two fragments are surrounded by the same transposable element, Tnp*1*, in pMEA02. Tnp*1* exhibited high levels of amino acid sequence identity (99% and 100%) with the IS*6100* transposase-like protein from the carbazole-degrading strain *Sphingomonas* sp. strain XLDN2-5 and *E. coli*, respectively (39).

There were no relevant hydroxylase genes in the 24,948-bp fragment encoding the proteins in spots A and B (data not shown); therefore, it was not analyzed in detail. A detailed search for ORFs in the 12,052-bp fragment revealed that *orf5*, encoding the hypothetical protein (HP1) in spot C, was an oxygenase gene (Table 4). Phylogenetic analysis showed that *orf5* encodes an amino acid sequence that shares significant identity with the oxygenase components of some two-component flavin-dependent monooxygenases (TC-FDMs) (Fig. 4); for example, HP1 exhibits 25% identity with C2-hpaH (*p*-hydroxyphenylacetate 3-hydroxylase) from *Acinetobacter baumannii* (40), 24% identity with HsaA [3-hydroxy-9,10-secoandrosta-1,3,5(10)-triene-9,17-dione monooxygenase] from *Rhodococcus* sp. strain RHA1 (41), and 22% identity with NcnH (naphthocyclinone hydroxylase) from *Streptomyces arenae* (42).

HsaA, NcnH, and C2-hpaH were previously classified as enzymes in the TC-FDM family, and the consensus sequences of this

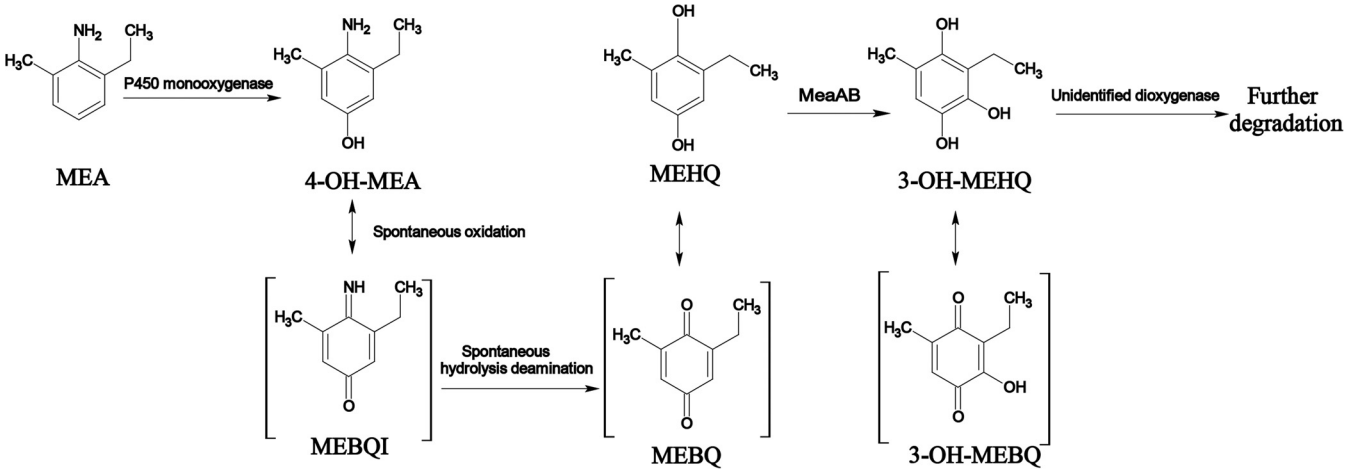

FIG 2 Partial metabolic pathway of MEA mineralization by *Sphingobium* sp. strain MEA3-1.

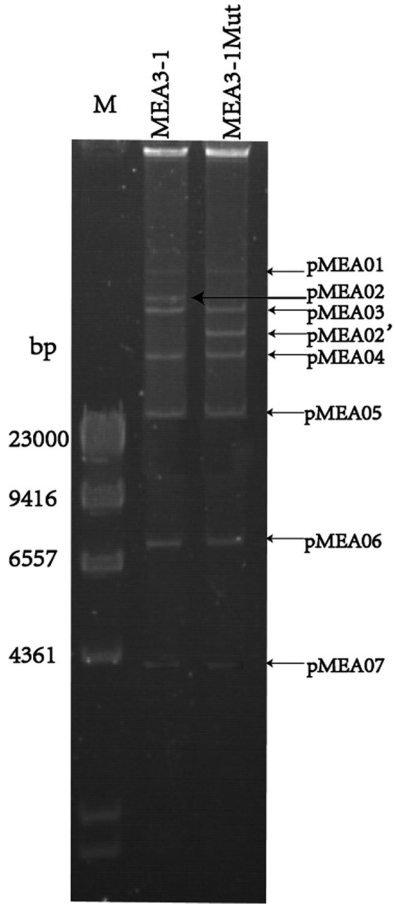

FIG 3 Plasmid profiles of strains MEA3-1 and MEA3-1Mut using PFGE. Lane M, HindIII digest of lambda phage DNA.

family were determined (43). HP1 has partially conserved residues (W86, W183, S145, W143, R264, H367, and M363) identical to residues in the consensus amino acid sequences interacting with flavin mononucleotide (FMN) in TC-FDM (see Fig. S5 in the supplemental material) (43). HP1 also contained the conserved domains COG1960 and KOG0139 belonging to the ACAD superfamily (44). These results indicate that HP1 is a novel oxygenase component of the TC-FDM family, and its absence in mutant MEA3-1Mut suggests that HP1 is responsible for the hydroxylation of MEHQ. *orf5* was designated *meaA* and encodes the oxygenase component MeaA of the MEHQ monooxygenase.

A BLAST analysis indicated that another hypothetical protein (HP2, encoded by *orf6*), located upstream of the *meaA* gene shared significant identity with cytochrome C (30% amino acid sequence identity with 40% coverage) from *Bacillus altitudinis*. We aligned HP2 with the reductase components of the TC-FDMs described above and found that the sequence identities with some hypothetical proteins ranged from 6 to 14% (40–42). We deduced that HP2 was the reduction component of a TC-FDM. The HP2 was assumed to be the reductase component of MeaA and was designated MeaB. The reductase component of the MEHQ hydroxylase (MeaB) may perform the NADH-dependent reduction of free FMN, which may be subsequently transferred to the larger

TABLE 4 Deduced functions of ORFs within the missing 12,052-bp fragment sequence

Gene	Product size (no. of amino acids)	Positions	Homologous protein	Source	GenBank accession no.	% amino acid identity
tnp1	264	1–795	Transposase IS*6100*	*E. coli*	YP_003108355.1	100
orf7	138	835–1251	Aminoglycoside phosphotransferase	*Sphingobium chlorophenolicum* L-1	YP_004554070.1	68
orf6 (*meaB*)	168	1251–1757	Hypothetical protein	*S. chlorophenolicum*	WP_013847811	31
orf5 (*meaA*)	392	2088–3266	Pigment production hydroxylase	*Rhodococcus opacus*	WP_012691790	39
orf1	480	3479–4921	Isopropylmalate isomerase large subunit	*Sphingomonas*-like bacterium B12	WP_022690399	81
orf2	199	4918–5517	Isopropylmalate isomerase small subunit	*S. chlorophenolicum*	WP_013849123	61
orf3	441	5727–7052	Homogentisate 1,2-dioxygenase	*Sphingomonas* sp. YL-JM2C	WP_037520129	52
orf4	123	7073–7444	Hypothetical protein Veis_4652	*Verminephrobacter eiseniae* EF01-2	YP_999367.1	58
orf8	284	6625–7479	Integrase catalytic subunit	*S. wittichii* RW1	YP_001260297.1	88
orf9	267	10253–11056	Putative transposase	*Magnetospirillum* sp. SO-1	WP_008622716.1	84
tnp1	264	12052–11258	Transposase IS*6100*	*E. coli*	YP_003108355.1	100

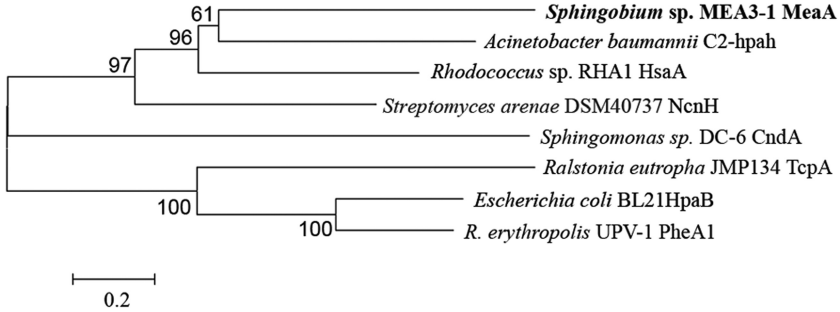

FIG 4 Neighbor-joining tree constructed using the alignment of MeaA with the amino acid sequences of the oxidation components of some characterized FDMs. The branches corresponding to partitions reproduced in <50% of the bootstrap replicates are collapsed. The names of the strains and proteins are displayed in the phylogenetic tree. The oxygenase components and their accession numbers are as follows: MeaA, KP752077; C2-hpaH, AY566612; HsaA, Q0S811; NcnH, AAG44124; TcpA, AAM55214; HpaB, YP003001901; PheA1, ABS30825; and CndA, KJ461679. CndA belongs to the oxygenase component of a Rieske non-heme iron monooxygenase and was used to provide a frame of reference for the phylogeny. *R. erythropolis*, *Rhodococcus erythropolis*.

monooxygenase component (MeaA) and used for MEHQ monooxygenation (Fig. 5C).

Functional expression of MeaBA. To further confirm the functions of MeaA, MeaB, and the products of the gene completely lacking the fragment (*meaBA-orf1-4*, excluding the transposable element), plasmids pBBR1MSC-2, pBBR-meaA, pBBR-meaBA, and pBBR-meaBA-orf1-4 were introduced into strains MEA3-1Mut, DH5α, and KT2440. The whole-cell transformation experiments revealed that strains MEA3-1Mut and KT2440 harboring pBBR-meaBA or pBBR-meaBA-orf1-4, but not pBBR-meaA, acquired the ability to degrade or transform MEHQ (Fig. 5A). The initial and final cell densities of strain MEA3-1Mut harboring pBBR-meaBA or pBBR-meaBA-orf1-4 were approximately 2×10^6 and 7.2×10^6 CFU/ml, respectively (Fig. 5B). In addition, strain KT2440 harboring pBBR-meaBA or pBBR-meaBA-orf1-4 acquired the ability to transform MEHQ but could not utilize MEHQ as a sole carbon source for growth (data not shown). Therefore, we confirmed that MeaBA contains the two components of the MEHQ monooxygenase, and *orf1* to *orf4* in the 12,052-bp fragment likely do not participate in the degradation of MEA. However, *E. coli* DH5α harboring either pBBR-meaBA or pBBR-meaBA-orf1-4 did not degrade MEHQ (Fig. 5A). This failure might be caused by codon usage, protein folding, or the low efficiency of the native *meaBA* promoter in *E. coli* DH5α (45). To exclude the third possibility, *meaBA* was placed under the control of a T7 promoter in the vector pET-29a(+) and introduced into *E. coli* BL21(DE3) (45). The results of the whole-cell transformation assay showed that isopropyl-β-D-thiogalactopyranoside (IPTG)-induced *E. coli* BL21(DE3) harboring pET29a-meaBAT7 was still unable to degrade MEHQ.

Possible enzyme involved in the upstream MEA metabolic pathway. We deduced that a P450 monooxygenase system initiates the degradation of MEA via aromatic ring hydroxylation at the *para* position. Metyrapone is a P450 inhibitor, and its effect on MEA degradation by strain MEA3-1 was tested (see Fig. S6 in the supplemental material). MEA degradation was visually observed, because MEA reacts with 4-aminoantipyrene to form a purple compound, and the color gradually deepens as MEA concentration increases. MEA degradation was inhibited when the metyrapone concentration was >200 mg/liter. These results show that a P450 monooxygenase system possibly initiates MEA degradation to transform MEA to 4-OH-MEA.

DISCUSSION

MEA and DEA are important degradation intermediates of several chloroacetanilide herbicides. Located on both sides of the amine group, the alkyl substituents of these aniline derivatives make their degradation processes different from that of anilines in natural soils (3, 10). Microbial degradation is an important process in the biogeochemical cycling and detoxification of organic pollutants in the environment. Several strains have been reported to degrade MEA, but the detailed degradation process is unclear (2, 10). It was proposed that DEA, a metabolite of butachlor, was degraded through dealkylation to an aniline, oxidation to a catechol, and ring cleavage through an *ortho*-cleavage pathway in *Paracoccus* sp. FLY-8 *in vitro* (9). In the present study, a novel flavin-dependent monooxygenase system for MEHQ hydroxylation, MeaBA, was cloned and characterized, and the possible metabolic pathway responsible for MEA degradation was proposed.

MEA was first transformed into the transitory intermediate 4-OH-MEA by a potential P450 monooxygenase. The degradation of DMA, a structural analogue of MEA, has been extensively studied in mammals (6, 14). It was reported that DMA was transformed to 4-OH-DMA in cultured mammalian cells by a P450 monooxygenase system (14). It has also been shown that the human cytochrome P450 isoforms responsible for the metabolism of alkylated aniline derivatives were CYP3A4 and CYP2B6 (6). Cytochrome P450 was proposed to be involved in the first degradation step of MEA by *Sphingobium* sp. MEA3-1. The cytochrome P450 inhibitor metyrapone (35) was found to inhibit the degradation of MEA by strain MEA3-1 (see Fig. S6 in the supplemental material). Therefore, we hypothesize that MEA is transformed into 4-OH-MEA in the presence of a P450 monooxygenase system. We found five cytochrome P450 oxygenases annotated in the genome of strain MEA3-1. A BLASTp analysis indicates that these cytochrome P450 oxygenases may be involved in the metabolism or synthesis of *N*-(1-pyrene)-acetamide, *N*-butyl-isocyanide, and cholesterol. However, whether they are involved in MEA degradation still needs to be clarified.

4-OH-MEA is an unstable intermediate that is oxidized rapidly to MEBQI in animals and microbes (10, 14). In this study, using Nessler's reagent to determine the release of ammonia from 4-OH-DMA (36), we found that MEBQI was spontaneously deaminated to MEHQ (see Fig. S2 in the supplemental material).

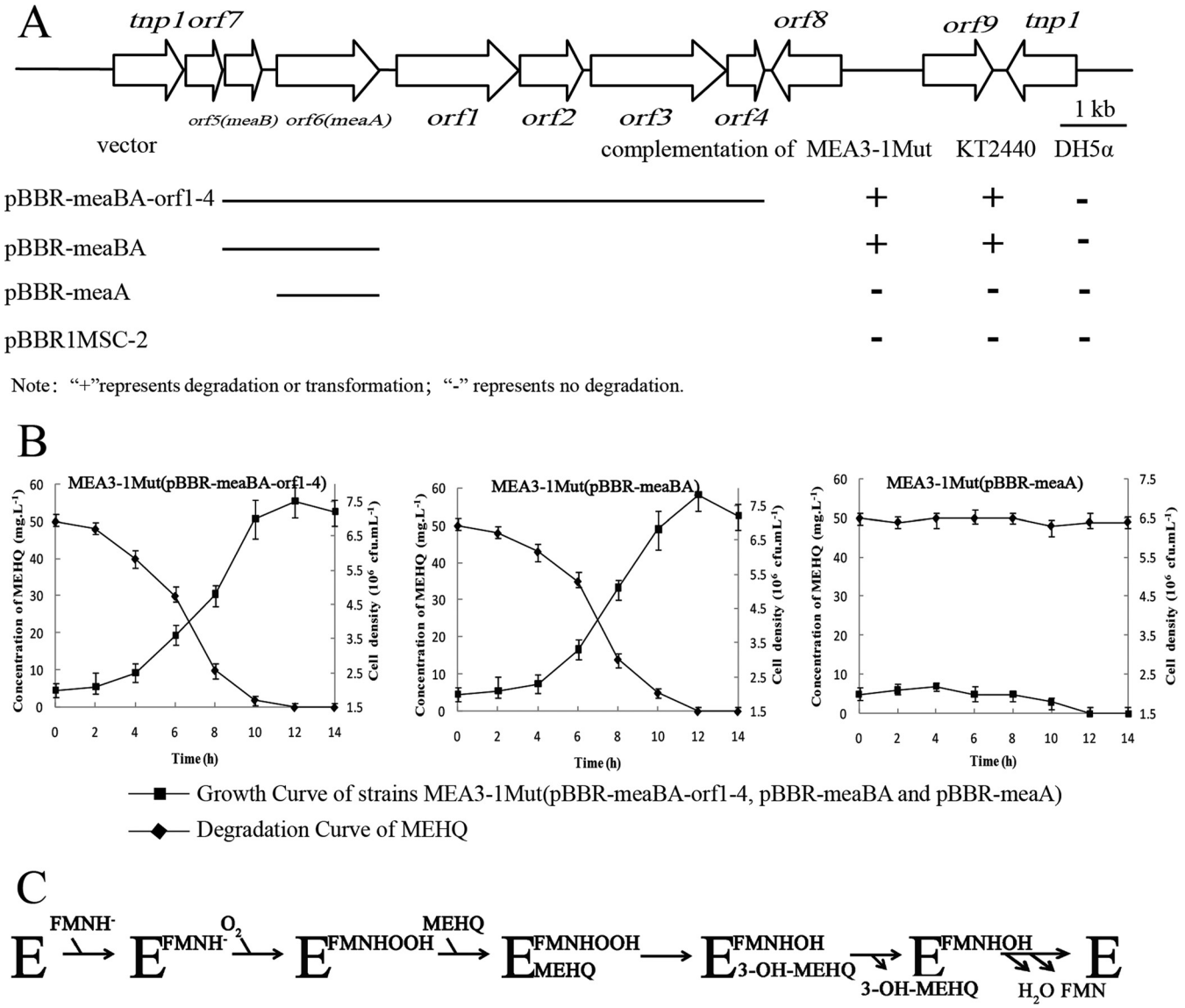

FIG 5 Physical map of the 12,052-bp putative transposable element containing *meaBA* in *Sphingobium* sp. strain MEA3-1. (A) Arrows indicate the sizes, locations, and directions of transcription of the ORFs. Complementation of the *meaBA*-disrupted mutants with different regions is illustrated below the physical map. (B) Degradation curve of MEHQ and the growth curve of MEA3-1Mut(pBBR-meaBA-orf1-4, pBBR-meaBA, and pBBR-meaA). (C) Probable scheme of the catalytic cycle of MEHQ hydroxylase MeaA. Error bars represent the standard deviations for three replicates.

Levenberg and Hayaishi (46) reported the hydrolytic deamination of the naturally occurring 2-amino-4-hydroxy-pteridines (pterins), which yielded the corresponding 2,4-dihydroxy compounds (lumazines). 4-OH-DMA, the degradation product of sulfonated azo dyes, was not observed in the reaction mixtures because it spontaneously and rapidly hydrolyzed to DMBQ (47).

Based on metabolite identification, MEHQ is further hydroxylated to form 3-OH-MEHQ (Fig. 1). Similar transformations have been reported in the degradation of xylenol compounds. Cell extracts of *Mycobacterium* sp. strain DM1 catalyzed the reduction of 2,6-dimethyl-3-hydroxyquinone (DMHQ) to 3-hydroxy-2,6-dimethyl-hydroquinone (3-OH-DMHQ) (48). Hofrichter et al. (49) also reported that the metabolism of DMHQ occurred via DMHQ, DMBQ, 3-OH-DMHQ, and 3-OH-DMBQ in *Penicillium frequentans* Bi7/2. However, the biotransformation mechanism of DMHQ and MEHQ to 3-OH-DMHQ and 3-OH-MEHQ, respectively, is still unclear.

In this study, using heterologous expression and complementation experiments, we identified two genes, *meaA* and *meaB*, that encode enzymes responsible for MEHQ hydroxylation. The oxygenase MeaA and reductase MeaB were obviously different from previously reported TC-FDMs at the amino acid sequence level, such as C2-hpaH (41), HsaAB (43), and NcnH (42). MeaB shared significant sequence identity with cytochrome *c* from *B. altitudinis*. The hydroxylation of 4-ethylphenol by the bacterial flavocytochrome *p*-cresol methylhydroxylase (PCMH) from *P. putida* has been proposed to be involved in the initial formation of an enzyme-bound *p*-quinone methide product intermediate (50, 51). The reductase component of MEHQ hydroxylase (MeaB) performs the NADH-dependent reduction of free FMN, which is

subsequently transferred to the larger monooxygenase component (MeaA) and used for the reaction of MEHQ monooxygenation (52).

Degradative plasmids are frequently isolated from *Sphingobium* species. Seven plasmid sequences (pMEA01 to pMEA07) were obtained from strain MEA3-1 (Fig. 3). Several instances of the degradation of aromatic compounds by genes carried on plasmids have been reported, such as those with pLB1 (a γ-hexachlorocyclohexane-degrading plasmid) from *Sphingobium japonicum* strain UT26 (53), pCF01-05 (a carbofuran-degrading plasmid) from *Sphingomonas* sp. strain CF06 (54), and pCAR3 (a carbazole-degrading plasmid) from *Sphingomonas* sp. strain KA1 (55). Until this study, Stolz (56) reported that, at most, five plasmids have been isolated from sphingomonads, namely, those found among two plasmids from *Sphingomonas aromaticivorans* strain F199, *Sphingomonas wittichii* strain RW1, and *Novosphingobium pentaromativorans* strain US6-1, three plasmids from *S. japonicum* strain UT26 and *Novosphingobium* sp. strain PP1Y, four plasmids from *Sphingomonas xenophagum* strain BN6 and *Sphingobium fuliginis* strain ATCC 27551, and five plasmids from *Sphingomonas* sp. strain MM-1 (56). The *meaBA* genes are located on plasmid pMEA02 and are surrounded by a transposable element from the IS*6100* family (Fig. 5A). This location might be the reason that MEA degradation was prone to loss.

The horizontal transfer of genes plays a key role in the evolution of catabolic pathways, thereby facilitating bacterial adaptation to pollutant-contaminated sites (57). Notably, many monooxygenase genes are associated with mobile genetic elements, such as IS*6100*, an insertion sequence classified in the IS*6* family. Wang et al. (58) reported that a novel 3-phenoxybenzoate 1,2-dioxygenase gene in *Sphingobium wenxiniae* strain JZ-1 was located between two IS*6100* transposase genes, *tnp1* and *tnp2*. Two identical nonylphenol monooxygenase genes were also surrounded by an IS*21*-type insertion sequence (IS) and IS*6100* in *Sphingomonas* sp. strain NP5 (59). Dogra et al. (60) revealed that most of the *lin* genes in *Sphingomonas paucimobilis* strains B90A, Sp+, and UT26 are associated with IS*6100*. Further research suggests that the IS*6100* elements have a very broad host range, and their presence on plasmids (even in strains in which their locations have not been ascertained) cannot be ruled out (60).

A downstream ring cleavage pathway and an initializing P450 monooxygenase still need to be identified in future research.

ACKNOWLEDGMENTS

This work was financially supported by the Natural Science Foundation of China (grants 31400098, 31270095, and 31560031), the National Basic Research Program (grant 2015CB1505002), the Natural Science Foundation of Jiangsu Province (grant BK2012029), the National Science and Technology Support Program (grants 2012BAD14B02 and 2014ZX08011-003), the 863 Project (grant 2013AA102804), and the Graduate Culture and Innovation Project of Jiangsu Province (grant KYLX_0514).

REFERENCES

1. **Foley ME, Sigler V, Gruden CL.** 2008. A multiphasic characterization of the impact of the herbicide acetochlor on freshwater bacterial communities. ISME J **2:**56–66. http://dx.doi.org/10.1038/ismej.2007.99.
2. **Hou Y, Dong W, Wang F, Li J, Shen W, Li Y, Cui Z.** 2014. Degradation of acetochlor by a bacterial consortium of *Rhodococcus* sp. T3-1, *Delftia* sp. T3-6 and *Sphingobium* sp. MEA3-1. Lett Appl Microbiol **59:**35–42.
3. **Chen Q, Wang CH, Deng SK, Wu YD, Li Y, Yao L, Jiang JD, Yan X, He J, Li SP.** 2014. Novel three-component Rieske non-heme iron oxygenase system catalyzing the *N*-dealkylation of chloroacetanilide herbicides in sphingomonads DC-6 and DC-2. Appl Environ Microbiol **80:**5078–5085. http://dx.doi.org/10.1128/AEM.00659-14.
4. **Xiao N, Jing B, Ge F, Liu X.** 2006. The fate of herbicide acetochlor and its toxicity to *Eisenia fetida* under laboratory conditions. Chemosphere **62:**1366–1373. http://dx.doi.org/10.1016/j.chemosphere.2005.07.043.
5. **Dearfield KL, McCarroll NE, Protzel A, Stack HF, Jackson MA, Waters MD.** 1999. A survey of EPA/OPP and open literature on selected pesticide chemicals: II. Mutagenicity and carcinogenicity of selected chloroacetanilides and related compounds. Mutat Res **443:**183–221.
6. **Coleman S, Linderman R, Hodgson E, Rose RL.** 2000. Comparative metabolism of chloroacetamide herbicides and selected metabolites in human and rat liver microsomes. Environ Health Perspect **108:**1151–1157. http://dx.doi.org/10.2307/3434827.
7. **Zhu JS, Qiao XW, Wang J, Qin S.** 2004. Degradation and the influencing factors of acetochlor in soils. J Agro-Environ Sci **23:**1025–1029.
8. **Souissi Y, Bourcier S, Ait-Aissa S, Maillot-Maréchal E, Bouchonnet S, Genty C, Sablier M.** 2013. Using mass spectrometry to highlight structures of degradation compounds obtained by photolysis of chloroacetamides: case of acetochlor. J Chromatogr A **1310:**98–112. http://dx.doi.org/10.1016/j.chroma.2013.07.091.
9. **Zhang J, Zheng JW, Liang B, Wang CH, Cai S, Ni YY, He J, Li SP.** 2011. Biodegradation of chloroacetanilide herbicides by *Paracoccus* sp. FLY-8 *in vitro*. J Agric Food Chem **59:**4614–4621. http://dx.doi.org/10.1021/jf104695g.
10. **Li Y, Chen Q, Wang CH, Cai S, He J, Huang X, Li SP.** 2013. Degradation of acetochlor by consortium of two bacterial strains and cloning of a novel amidase gene involved in acetochlor-degrading pathway. Bioresour Technol **148:**628–631. http://dx.doi.org/10.1016/j.biortech.2013.09.038.
11. **Wang F, Zhou J, Li Z, Dong W, Hou Y, Huang Y, Cui Z.** 2015. Involvement of the cytochrome P450 system EthBAD in the *N*-deethoxymethylation of acetochlor by *Rhodococcus* sp. strain T3-1. Appl Environ Microbiol **81:**2182–2188.
12. **Wang F, Hou Y, Zhou J, Li Z, Huang Y, Cui Z.** 2014. Purification of an amide hydrolase DamH from *Delftia* sp. T3-6 and its gene cloning, expression, and biochemical characterization. Appl Microbiol Biotechnol **98:**7491–7499.
13. **Boonrattanakij N, Lu MC, Anotai J.** 2009. Kinetics and mechanism of 2,6-dimethyl-aniline degradation by hydroxyl radicals. J Hazard Mater **172:**952–957. http://dx.doi.org/10.1016/j.jhazmat.2009.07.079.
14. **Chao MW, Kim MY, Ye W, Ge J, Trudel LJ, Belanger C, Wogan GN.** 2012. Genotoxicity of 2,6- and 3,5-dimethylaniline in cultured mammalian cells: the role of reactive oxygen species. Toxicol Sci **130:**48–59.
15. **Sambrook J, Russell DW.** 2001. Molecular cloning: a laboratory manual, 3rd ed. Cold Spring Harbor Laboratory Press, Cold Spring Harbor, NY.
16. **Endo R, Kamakura M, Miyauchi K, Fukuda M, Ohtsubo Y, Tsuda M, Nagata Y.** 2005. Identification and characterization of genes involved in the downstream degradation pathway of γ-hexachlorocyclohexane in *Sphingomonas paucimobilis* UT26. J Bacteriol **187:**847–853. http://dx.doi.org/10.1128/JB.187.3.847-853.2005.
17. **de Bruijn FJ.** 1992. Use of repetitive (repetitive extragenic palindromic and enterobacterial repetitive intergeneric consensus) sequences and the polymerase chain reaction to fingerprint the genomes of *Rhizobium meliloti* isolates and other soil bacteria. Appl Environ Microbiol **58:**2180–2187.
18. **O'Sullivan DJ, Klaenhammer TR.** 1993. Rapid mini-prep isolation of high-quality plasmid DNA from *Lactococcus* and *Lactobacillus* spp. Appl Environ Microbiol **59:**2730–2733.
19. **Kaufmann ME.** 1998. Pulsed-field gel electrophoresis. Mol Bacteriol **15:**33–50. http://dx.doi.org/10.1385/0-89603-498-4:33.
20. **Castoe TA, Poole AW, Gu W, Jason de Koning AP, Daza JM, Smith EN, Pollock DD.** 2010. Rapid identification of thousands of copperhead snake (*Agkistrodon contortrix*) microsatellite loci from modest amounts of 454 shotgun genome sequence. Mol Ecol Resour **10:**341–347. http://dx.doi.org/10.1111/j.1755-0998.2009.02750.x.
21. **Ansorge WJ.** 2009. Next-generation DNA sequencing techniques. New Biotechnol **25:**195–203. http://dx.doi.org/10.1016/j.nbt.2008.12.009.
22. **Altschul SF, Gish W, Miller W, Myers EW, Lipman DJ.** 1990. Basic Local Alignment Search Tool. J Mol Biol **215:**403–410. http://dx.doi.org/10.1016/S0022-2836(05)80360-2.
23. **Tang B, Wang Q, Yang M, Xie F, Zhu Y, Zhuo Y, Wang S, Gao H, Ding X, Zhang L, Zhao G, Zheng H.** 2013. ContigScape: a Cytoscape plugin

facilitating microbial genome gap closing. BMC Genomics **14:**289. http://dx.doi.org/10.1186/1471-2164-14-289.
24. **Wang S, He J, Cui Z, Li S.** 2007. Self-formed adaptor PCR: a simple and efficient method for chromosome walking. Appl Environ Microbiol **73:**5048–5051. http://dx.doi.org/10.1128/AEM.02973-06.
25. **Ramagli LS.** 1999. Quantifying protein in 2-D PAGE solubilization buffers. Methods Mol Biol **112:**99–103.
26. **Song Y, Cui J, Zhang H, Wang G, Zhao FJ, Shen Z.** 2013. Proteomic analysis of copper stress responses in the roots of two rice (*Oryza sativa* L.) varieties differing in Cu tolerance. Plant Soil **366:**647–658. http://dx.doi.org/10.1007/s11104-012-1458-2.
27. **Yan JX, Wait R, Berkelman T, Harry RA, Westbrook JA, Wheeler CH, Dunn MJ.** 2000. A modified silver staining protocol for visualization of proteins compatible with matrix-assisted laser desorption/ionization and electrospray ionization-mass spectrometry. Electrophoresis **21:**3666–3672. http://dx.doi.org/10.1002/1522-2683(200011)21:17<3666::AID-ELPS3666>3.0.CO;2-6.
28. **Larkin M, Blackshields G, Brown N, Chenna R, McGettigan PA, McWilliam H, Valentin F, Wallace IM, Wilm A, Lopez R, Thompson JD, Gibson TJ, Higgins DG.** 2007. Clustal W and Clustal X version 2.0. Bioinformatics **23:**2947–2948. http://dx.doi.org/10.1093/bioinformatics/btm404.
29. **Tamura K, Peterson D, Peterson N, Stecher G, Nei M, Kumar S.** 2011. MEGA5: Molecular Evolutionary Genetics Analysis using maximum likelihood, evolutionary distance, and maximum parsimony methods. Mol Biol Evol **28:**2731–2739. http://dx.doi.org/10.1093/molbev/msr121.
30. **Kovach ME, Elzer PH, Hill DS, Robertson GT, Farris MA, Roop RM, Jr, Peterson KM.** 1995. Four new derivatives of the broad-host-range cloning vector pBBR1MCS, carrying different antibiotic-resistance cassettes. Gene **166:**175–176. http://dx.doi.org/10.1016/0378-1119(95)00584-1.
31. **Martínez-García E, Jatsenko T, Kivisaar M, de Lorenzo V.** 2014. Freeing *Pseudomonas putida* KT2440 of its proviral load strengthens endurance to environmental stresses. Environ Microbiol **17:**76–90.
32. **Li J, Huang Y, Hou Y, Li X, Cao H, Cui Z.** 2013. Novel gene clusters and metabolic pathway involved in 3,5,6-trichloro-2-pyridinol degradation by *Ralstonia* sp. strain T6. Appl Environ Microbiol **79:**7445–7453. http://dx.doi.org/10.1128/AEM.01817-13.
33. **Glazebrook J, Walker GC.** 1991. Genetic techniques in *Rhizobium meliloti*. Methods Enzymol **204:**398–418. http://dx.doi.org/10.1016/0076-6879(91)04021-F.
34. **Liu H, Wang SJ, Zhang JJ, Dai H, Tang H, Zhou NY.** 2011. Patchwork assembly of nag-like nitroarene dioxygenase genes and the 3-chlorocatechol degradation cluster for evolution of the 2-chloronitrobenzene catabolism pathway in *Pseudomonas stutzeri* ZWLR2-1. Appl Environ Microbiol **77:**4547–4552. http://dx.doi.org/10.1128/AEM.02543-10.
35. **Sasaki M, Maki JI, Oshiman KI, Matsumura Y, Tsuchido T.** 2005. Biodegradation of bisphenol A by cells and cell lysate from *Sphingomonas* sp. strain AO1. Biodegradation **16:**449–459. http://dx.doi.org/10.1007/s10532-004-5023-4.
36. **Lin YM, Li LY, Hu JW, Huang XF, Zhou C, Jia M, Li ZB.** 2014. Photometric determination of ammonia nitrogen in slaughterhouse wastewater with Nessler's reagent: effects of different pretreatment methods. Adv Mater **955:**1241–1244.
37. **Gillings M, Holley M.** 1997. Repetitive element PCR fingerprinting (rep-PCR) using enterobacterial repetitive intergenic consensus (ERIC) primers is not necessarily directed at ERIC elements. Lett Appl Microbiol **25:**17–21. http://dx.doi.org/10.1046/j.1472-765X.1997.00162.x.
38. **Zhang T, Zhang J, Liu S, Liu Z.** 2008. A novel and complete gene cluster involved in the degradation of aniline by *Delftia* sp. AN3. J Environ Sci **20:**717–724. http://dx.doi.org/10.1016/S1001-0742(08)62118-X.
39. **Gai Z, Wang X, Liu X, Tai C, Tang H, He X, Xu P.** 2010. The genes coding for the conversion of carbazole to catechol are flanked by IS*6100* elements in *Sphingomonas* sp. strain XLDN2-5. PLoS One **5:**e10018. http://dx.doi.org/10.1371/journal.pone.0010018.
40. **Thotsaporn K, Sucharitakul J, Wongratana J, Suadee C, Chaiyen P.** 2004. Cloning and expression of *p*-hydroxyphenylacetate 3-hydroxylase from *Acinetobacter baumannii*: evidence of the divergence of enzymes in the class of two-protein component aromatic hydroxylases. Biochim Biophys Acta **1680:**60–66. http://dx.doi.org/10.1016/j.bbaexp.2004.08.003.
41. **Van der Geize R, Yam K, Heuser T, Wilbrink MH, Hara H, Anderton MC, Sim E, Dijkhuizen L, Davies JE, Mohn WW, Eltis LD.** 2007. A gene cluster encoding cholesterol catabolism in a soil actinomycete provides insight into *Mycobacterium tuberculosis* survival in macrophages. Proc Natl Acad Sci U S A **104:**1947–1952. http://dx.doi.org/10.1073/pnas.0605728104.
42. **Brünker P, Sterner O, Bailey JE, Minas W.** 2001. Heterologous expression of the naphthocyclinone hydroxylase gene from *Streptomyces arenae* for production of novel hybrid polyketides. Antonie Van Leeuwenhoek **79:**235–245. http://dx.doi.org/10.1023/A:1012037329949.
43. **Galán B, Díaz E, Prieto MA, García JL.** 2000. Functional analysis of the small component of the 4-hydroxyphenylacetate 3-hydroxylase of *Escherichia coli* W: a prototype of a new flavin: NAD(P)H reductase subfamily. J Bacteriol **182:**627–636. http://dx.doi.org/10.1128/JB.182.3.627-636.2000.
44. **Thompson JD, Higgins DG, Gibson TJ.** 1994. CLUSTAL W: improving the sensitivity of progressive multiple sequence alignment through sequence weighting, position-specific gap penalties and weight matrix choice. Nucleic Acids Res **22:**4673–4680. http://dx.doi.org/10.1093/nar/22.22.4673.
45. **Gu T, Zhou C, Sørensen SR, Zhang J, He J, Yu P, Yan X, Li S.** 2013. The novel bacterial *N*-demethylase PdmAB is responsible for the initial step of *N*,*N*-dimethyl-substituted phenylurea herbicide degradation. Appl Environ Microbiol **79:**7846–7856. http://dx.doi.org/10.1128/AEM.02478-13.
46. **Levenberg B, Hayaishi O.** 1959. A bacterial pterin deaminase. J Biol Chem **234:**955–961.
47. **Goszczynski S, Paszczynski A, Pasti-Grigsby MB, Crawford RL, Crawford DL.** 1994. New pathway for degradation of sulfonated azo dyes by microbial peroxidases of *Phanerochaete chrysosporium* and *Streptomyces chromofuscus*. J Bacteriol **176:**1339–1347.
48. **Ewers J, Rubio MA, Knackmuss HJ, Freier-Schröder D.** 1989. Bacterial metabolism of 2,6-xylenol. Appl Environ Microbiol **55:**2904–2908.
49. **Hofrichter M, Bublitz F, Fritsche W.** 1995. Cometabolic degradation of *o*-cresol and 2,6-dimethylphenol by *Penicillium frequentans* Bi7/2. J Basic Microbiol **35:**303–313. http://dx.doi.org/10.1002/jobm.3620350505.
50. **McIntire WS, Bohmont C.** 1987. The chemical and stereochemical course of oxidation of 4-ethylphenol and other 4-alkylphenols by *p*-cresol methylhydroxylase, p 677–686. *In* Edmondson DE, McCormick DB (ed), Flavins and flavoproteins IX. Walter de Gruyter, Berlin, Germany.
51. **Reeve CD, Carver MA, Hopper DJ.** 1990. Stereochemical aspects of the oxidation of 4-ethylphenol by the bacterial enzyme 4-ethylphenol methylenehydroxylase. Biochem J **269:**815–819. http://dx.doi.org/10.1042/bj2690815.
52. **Alfieri A, Fersini F, Ruangchan N, Prongjit M, Chaiyen P, Mattevi A.** 2007. Structure of the monooxygenase component of a two-component flavoprotein monooxygenase. Proc Natl Acad Sci U S A **104:**1177–1182. http://dx.doi.org/10.1073/pnas.0608381104.
53. **Miyazaki R, Sato Y, Ito M, Ohtsubo Y, Nagata Y, Tsuda M.** 2006. Complete nucleotide sequence of an exogenously isolated plasmid, pLB1, involved in γ-hexachlorocyclohexane degradation. Appl Environ Microbiol **72:**6923–6933. http://dx.doi.org/10.1128/AEM.01531-06.
54. **Feng X, Ou LT, Ogram A.** 1997. Plasmid-mediated mineralization of carbofuran by *Sphingomonas* sp. strain CF06. Appl Environ Microbiol **63:**1332–1337.
55. **Shintani M, Urata M, Inoue K, Eto K, Habe H, Omori T, Yamane H, Nojiri H.** 2007. The *Sphingomonas* plasmid pCAR3 is involved in complete mineralization of carbazole. J Bacteriol **189:**2007–2020. http://dx.doi.org/10.1128/JB.01486-06.
56. **Stolz A.** 2014. Degradative plasmids from sphingomonads. FEMS Microbiol Lett **350:**9–19. http://dx.doi.org/10.1111/1574-6968.12283.
57. **Liang B, Wang G, Zhao Y, Chen K, Li S, Jiang J.** 2011. Facilitation of bacterial adaptation to chlorothalonil-contaminated sites by horizontal transfer of the chlorothalonil hydrolytic dehalogenase gene. Appl Environ Microbiol **77:**4268–4272. http://dx.doi.org/10.1128/AEM.02457-10.
58. **Wang C, Chen Q, Wang R, Shi C, Yan X, He J, Hong Q, Li S.** 2014. A novel angular dioxygenase gene cluster encoding 3-phenoxybenzoate 1′,2′-dioxygenase in *Sphingobium wenxiniae* JZ-1. Appl Environ Microbiol **80:**3811–3818. http://dx.doi.org/10.1128/AEM.00208-14.
59. **Takeo M, Maeda Y, Maeda J, Nishiyama N, Kitamura C, Kato DI, Negoro S.** 2012. Two identical nonylphenol monooxygenase genes linked to IS*6100* and some putative insertion sequence elements in *Sphingomonas* sp. NP5. Microbiology **158:**1796–1807. http://dx.doi.org/10.1099/mic.0.055335-0.
60. **Dogra C, Raina V, Pal R, Suar M, Lal S, Gartemann KH, Holliger C, van der Meer JR, Lal R.** 2004. Organization of *lin* genes and IS*6100* among different strains of hexachlorocyclohexane-degrading *Sphingomonas paucimobilis*: evidence for horizontal gene transfer. J Bacteriol **186:**2225–2235. http://dx.doi.org/10.1128/JB.186.8.2225-2235.2004.